5ème Conférence Internationale des Energies Renouvelables (CIER– 2017)
Proceeding of Engineering and Technology –PET
Vol.28 pp.57-61

Numeric modelling of a low temperature plasma setup

G. BARKAOUI[#1], N. JOMAA[#2], K CHARRDA[#3]
[#]*Ionized and Reactive Media Studies Research Unit,*
Preparatory Institute of Engineering Studies of Monastir,
Monastir University, Ibn Eljazar Avenue, Monastir 5019, Tunisia
[1]ghadabarkaoui91@yahoo.fr
[3]Kamel.Charrada@ipeim.rnu.tn
[2]neil.jomaa@gmail.com

Abstract: The aim is to do a numeric modeling of a low temperature plasma source for biomedical applications. The plasma is generated at atmospheric pressure by dielectric barrier discharge (DBD) setup using an argon carrier gas. The dilution of the argon in air is simulated by a hydrodynamic model based on the Navier-Stokes equation including diffusion flows in a mixture simulates the dilution of the argon in air, the simulation of the plasma jet is formed by the Poisson equation and the conservation equations of charged particles. The reactions between electron and the ions present in Ar-air mixtures is taken into account with their basic data (transport and reaction coefficients). The study is based on the finite element method for discretization using the COMSOL Multiphysics software.

Keywords: Low-temperature plasma, Dielectric barrier discharges, atmospheric pressure.

1. Introduction

Low-temperature plasmas generated at atmospheric pressure are very useful in the field of biological and medical applications due to their ability to form an important population of active species without the need to elevate gas temperature. Food processing[1], Inactivation of different microorganisms[2], Blood coagulation[3], wound healing[4] and cancer treatment[5] are some of this biological and medical applications.

There are many ways to generate atmospheric pressure plasma jet such Dielectric barrier discharges (DBD)[6], Radio frequency (RF)[7] and Microwave plasmas (MW)[8], many carrier gas can be used too (He, Ar, Ne, Air and mixture of inert gases with air). The DBD setup is more suitable for the biomedical applications because of his ability to generate plasma with moderate temperature and electronic density.

To more understand the physics and the applications of low temperature plasmas, reader can find many works in the literature[9–13]. Many proprieties of cold plasma jet have been studied: Gas flow velocity, applied voltage, jet radius, geometries [14–17].

The present work presents a numeric simulation of low temperature plasma generated by dielectric barrier discharge (DBD) using an argon carrier gas, formed in a glass tube and ejected into open air. An experimental investigation with the same conditions (tube size, electrode geometry, pulse duration, argon flow rate, voltage) was revealed in literature [17].

2. The model

The DBD jet configuration used in this work, shown in Fig 1, consists of a quartz tube with an external diameter of 8 mm, an internal diameter of 6 mm and a length of 60 mm and wrapped by a ring ground electrode, which is

***Corresponding author:** Ghada BARKAOUI
E-mail: ghadabarkaoui91@yahoo.fr

ISSN 2356-5608

composed of aluminum and located at 6 mm away from the outlet of the tube. The high voltage (HV) electrode made of copper have a diameter of 2 mm and positioned along the axis of the quartz tube. The argon is ejected from another quartz tube of 6 mm outer diameter and 1 mm thickness positioned at 7 mm away from the inlet of the first tube.

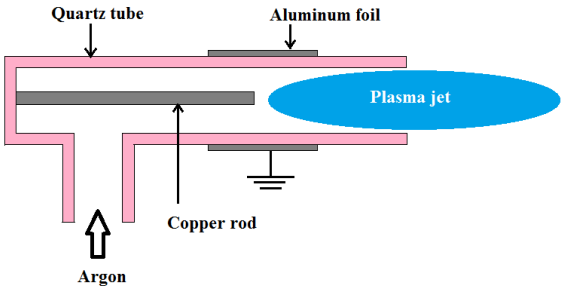

Fig. 1 Schematic overview of the setup for generating and launching a plasma jet in open air

To estimate the argon dilution in air, a hydrodynamics model was used, this model was based on the Navier-Stokes equations (1-2) in which we consider a stationary and laminar flow, the transport of the argon into the air is assured by two phenomena: convection and diffusion, the equation of the transport in our case is taken into account in static mode (3). The gas flow was set under 4l/min to maintain a Reynolds number under 1000.

$$\vec{\nabla}(\vec{u}) = 0 \qquad (1)$$

$$\rho(\vec{u}\,\vec{\nabla})\vec{u} = -\vec{\nabla}p + \mu\vec{\Delta}\vec{u} \qquad (2)$$

$$\vec{u}\,\vec{\nabla}c = \vec{\nabla}(D\,\vec{\nabla}c) \qquad (3)$$

The initial geometrical electric field is at the origin of the initial wave front, which initiates the electronic avalanche. This electrostatic model is based on the Laplace equation (4,5) and the transition relation (6).

$$\nabla^2 V = 0 \qquad (4)$$

$$\vec{E} = -\vec{\nabla}.V \qquad (5)$$

$$\overrightarrow{D1} - \overrightarrow{D2} = \vec{0} \qquad (6)$$

The plasma model is based on conservation equations of charged particles coupled to Poisson equation (10,11).

- For electrons

$$\frac{\partial ne}{\partial t} + \vec{\nabla}\overrightarrow{\Gamma e} = R_e - (\vec{u}.\vec{\nabla})n_e \qquad (7)$$

- For heavy species

$$\rho\frac{\partial w_j}{\partial t} = \vec{\nabla}\overrightarrow{\Gamma k} + R_j \qquad (8)$$

- Equation of conservation of electronic energy

$$\frac{\partial n_\varepsilon}{\partial t} + \vec{\nabla}\overrightarrow{\Gamma\varepsilon} + \vec{E}.\overrightarrow{\Gamma e} = R_\varepsilon - (\vec{u}.\vec{\nabla})\,n_\varepsilon \qquad (9)$$

- Poisson equation

$$\nabla^2.V = -\frac{\rho_v}{\varepsilon_0} \qquad (10)$$

Table 1. Interaction processes considered in the model with their rate constants

Nr	Reaction name	Rate constants [$m^3.s^{-1}.mol^{-1}$]
1	$e + O2 \rightarrow O + O^-$	$k_1 = fct(x_{Ar},\varepsilon)^*$
2	$e + O_2 \rightarrow 2e + O_2^+$	$k_2 = fct(x_{Ar},\varepsilon)^*$
3	$e + N_2 \rightarrow 2e + N_2^+$	$k_3 = fct(x_{Ar},\varepsilon)^*$
4	$e + Ar \rightarrow 2e + Ar^+$	$k_4 = fct(x_{Ar},\varepsilon)^*$
5	$e + Ar \rightarrow e + Ar^*$	$k_5 = fct(x_{Ar},\varepsilon)^*$
6	$e + Ar^* \rightarrow 2e + Ar^+$	$k_6 = fct(x_{Ar},\varepsilon)^*$
7	$2e + Ar^+ \Rightarrow e + Ar^*$	$K_7 = 5.10^{-32}.Te^{-4.5}$ [18]
8	$e + Ar^+ \Rightarrow Ar^*$	$K_8 = 4.10^{-19}.Te^{-0.5}$ [18]
9	$e+Ar_2^* \Rightarrow 2e+Ar_2^+$	$k_9=9.10^{-14}.Te.\exp(\frac{-3.66}{Te})$ [18]
10	$e+Ar_2^+ \Rightarrow Ar^*+Ar$	$k_{10} = 5{,}38.10^{-14}.Te^{-0.66}$ [18]
11	$Ar^+ + Ar+Ar \Rightarrow Ar+Ar_2^*$	$k_{11} = 2{,}5.10^{-32}$ [18]
12	$Ar_2^+ + O^- \Rightarrow O + Ar$	$k_{12} = 10^{-13}$ [18]
13	$Ar^+ + O^- \Rightarrow O + Ar$	$k_{12} = 10^{-13}$ [18]

*Calculated within LAPLACE

The plasma in our model results from the ionization of the gas mixture formed by the progressive dilution of the Ar ejected from the tube in the ambient air. It is assumed that the air is mainly formed by the oxygen O_2 and the nitrogen N_2 and neglects the impurities and the humidity. We considered the formation of the positives ions: Ar^+, N_2^+

O_2^+ and Ar_2^+ and the negative ion O-, we considered also the presence of the metastable state of argon (formed by the reaction 5 in table 1), the ionization of both metastable and background states of Ar was taken into account to be able to propagate the plasma jet for the relatively low electric field values.

The ionization energy of the background state of Ar is 15.76 eV, the excitation energy of Ar is 11.5 and the ionization energy of Ar metastable states is 15.76 – 11.5 = 4.26 eV.

To simulate the ionization wave propagation and development, the finite element method for discretization is applied, using the COMSOL Multiphysics software.

Several tests were carried out in order to choose the right mesh size.

3. Results and discussion

- Hydrodynamic results

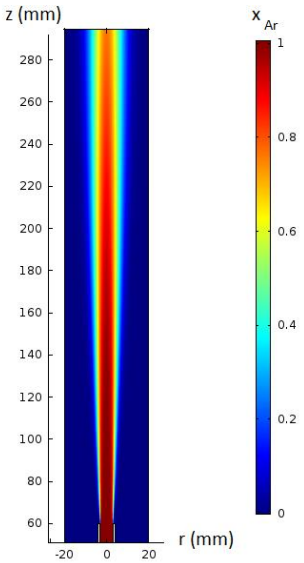

Fig. 2 Reduced argon concentration from the exit of the tube for argon gas velocity: 2.56 m/s

Fig.2 shows that the molar fraction takes the form of a beam and it decreases as it moves away from the tube outlet, it shows also that the radial dilution is faster than the axial dilution.

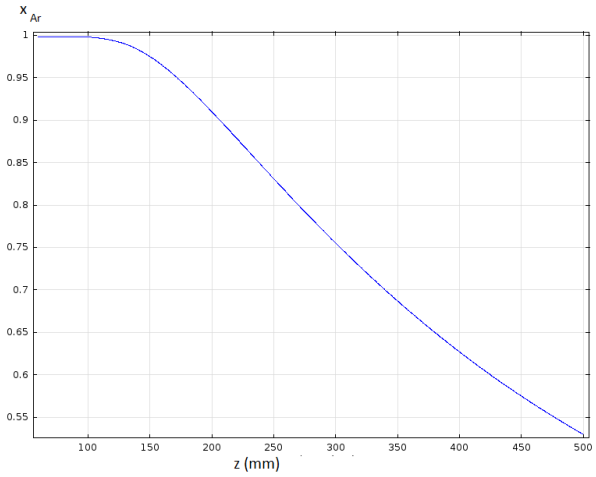

Fig. 3 Reduced argon concentration from the exit of the tube along the tube axisfor r = 0 mm and for argon gas velocity: 2.56 m/s

The profile 1d of the molar fraction shown in Fig.3 shows that the molar fraction remains constant over a distance of 40 mm from the outlet of the tube, the jet consists of pure argon over this distance, and then the gas begins to dilute in air.

- Electrostatic results

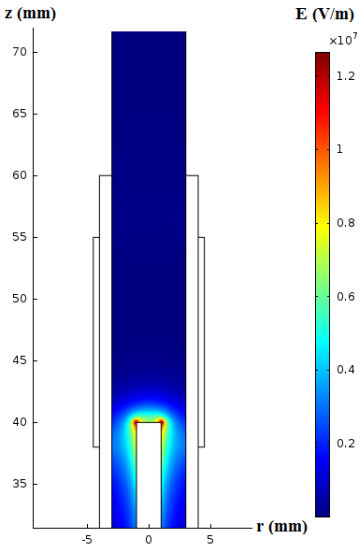

Fig. 4 Electric field for V_0 = 10 kV

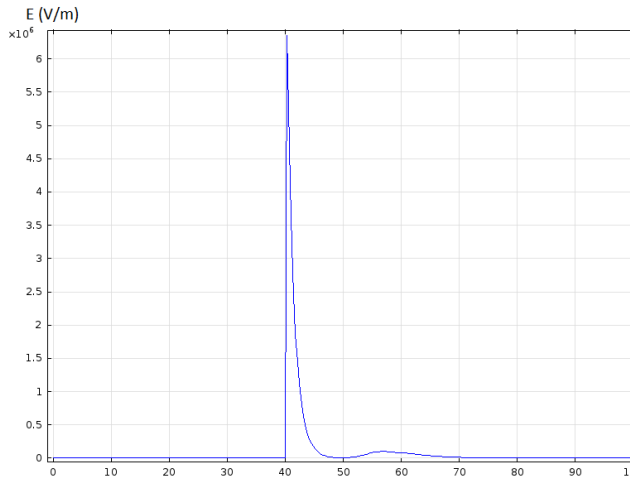

Fig.5 Axially electric field along the tube axis for r=0 and V_0 = 10 kV

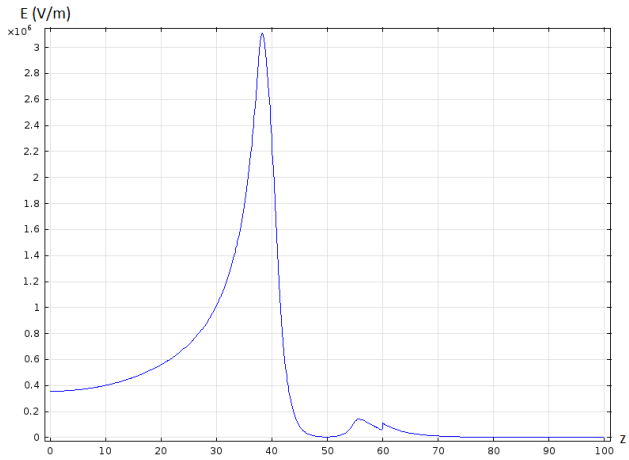

Fig. 6 Axially electric field along the tube axis for r = 2.9 mm and V_0 = 10 kV

Fig 5 and Fig 6 show that the profile of the electric field is composed of a first peak, which is the initiator of the plasma jet; this peak is followed by a secondary peak at the outlet of the tube due to the polarization of the dielectric material.

- Electrodynamics results

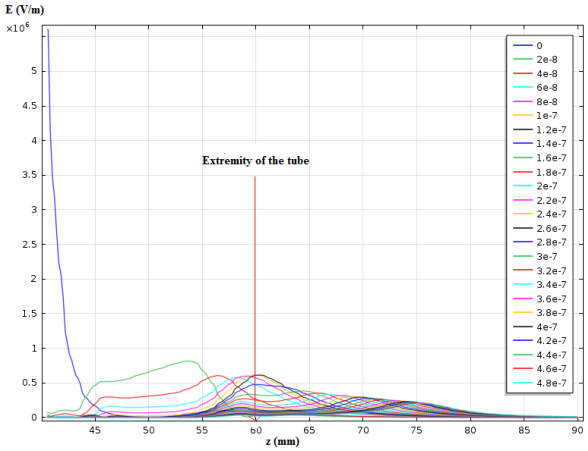

Fig. 7 Axially electric field along the tube axis for r=0 and V_0 = 10 kV.

The first peak, showed in Fig(7) in blue, correspond to the geometric electric field. At t = 20 ns, the maximum of the electric field was placed towards z = 53.3 mm and the peak begins to split into two other peaks, one tends to propagate towards the extremity of the tube and the other tends to propagate towards the opposite direction. At t = 120 ns, the maximum of the electric field is located at the extremity of the tube (z = 60 mm). At 480 ns the electric field reaches the position z = 75 mm.

4. Conclusion

This work allowed us to predict the profile of the electric field that propagate in Ar-air mixture.

References

[1] R. Thirumdas, C. Sarangapani, and U. S. Annapure, "Cold Plasma: A novel Non-Thermal Technology for Food Processing," *Food Biophys.*, vol. 10, no. 1, pp. 1–11, Mar. 2015.

[2] T. M. C. Nishime, A. C. Borges, C. Y. Koga-Ito, M. Machida, L. R. O. Hein, and K. G. Kostov, "Non-thermal atmospheric pressure plasma jet applied to inactivation of different microorganisms," *Surf. Coat. Technol.*, vol. 312, no. Supplement C, pp. 19–24, Feb. 2017.

[3] S. U. Kalghatgi *et al.*, "Mechanism of Blood Coagulation by Nonthermal Atmospheric Pressure Dielectric Barrier Discharge Plasma," *IEEE Trans. Plasma Sci.*, vol. 35, no. 5, pp. 1559–1566, Oct. 2007.

[4] S. Bekeschus, A. Schmidt, K.-D. Weltmann, and T. von Woedtke, "The plasma jet kINPen – A powerful tool for wound healing," *Clin. Plasma Med.*, vol. 4, no. 1, pp. 19–28, Jul. 2016.

[5] A. M. Hirst, F. M. Frame, N. J. Maitland, and D. Connell, "Low Temperature Plasma: A Novel Focal Therapy for Localized Prostate Cancer?," *BioMed Research International*, 2014.

[6] U. Kogelschatz, "Dielectric-Barrier Discharges: Their History, Discharge Physics, and Industrial Applications," *Plasma Chem. Plasma Process.*, vol. 23, no. 1, pp. 1–46, Mar. 2003.

[7] J. Park, I. Henins, H. W. Herrmann, G. S. Selwyn, and R. F. Hicks, "Discharge phenomena of an atmospheric pressure radio-frequency capacitive plasma source," *J. Appl. Phys.*, vol. 89, no. 1, pp. 20–28, Dec. 2000.

[8] G. Wattieaux, M. Yousfi, N. Merbahi, G, "Optical emission spectroscopy for quantification of ultraviolet radiations and biocide active species in microwave argon plasma jet at atmospheric pressure,"*ScienceDirect*, vol. 89, pp 66-76, Nov. 2013.

[9] J. Florian, N. Merbahi, G. Wattieaux, J. M . Plewa, M.Yousfi, "Comparative Studies of Double Dielectric Barrier Discharge and Microwave Argon Plasma Jets at Atmospheric Pressure for Biomedical Applications," *IEEE Trans. Plasma Sci.*, vol. 43, no. 2, pp. 3332-3338, March 2015.

[10] A. Shashurin, M. N. Shneider, A. Dogariu, R. B. Miles, and M. Keidar, "Temporal behavior of cold atmospheric plasma jet," *Appl. Phys. Lett.*, vol. 94, no. 23, p. 231504, Jun. 2009.

[11] D. B. Graves, "Mechanisms of Plasma Medicine: Coupling Plasma Physics, Biochemistry, and Biology," *IEEE Trans. Radiat. Plasma Med. Sci.*, vol. 1, no. 4, pp. 281–292, Jul. 2017.

[12] J. A. Bittencourt, *Fundamentals of Plasma Physics*. Springer Science & Business Media, 2013.

[13] M. Laroussi, X. Lu, and M. Keidar, "Perspective: The physics, diagnostics, and applications of atmospheric pressure low temperature plasma sources used in plasma medicine," *J. Appl. Phys.*, vol. 122, no. 2, p. 020901, Jul. 2017.

[14] N. Jiang, A. Ji, and Z. Cao, "Atmospheric pressure plasma jet: Effect of electrode configuration, discharge behavior, and its formation mechanism," *J. Appl. Phys.*, vol. 106, no. 1, p. 013308, Jul. 2009.

[15] M. Yousfi, O. Eichwald, N. Merbahi, and N. Jomaa, "Analysis of ionization wave dynamics in low-temperature plasma jets from fluid modeling supported by experimental investigations," *Plasma Sources Sci. Technol.*, vol. 21, no. 4, p. 045003, 2012.

[16] C. L. Enloe *et al.*, "Mechanisms and Responses of a Dielectric Barrier Plasma Actuator: Geometric Effects," *AIAA J.*, vol. 42, no. 3, pp. 595–604, 2004.

[17] F. Judée, N. Merbahi, G. Wattieaux, and M. Yousfi, "Analysis of Ar plasma jets induced by single and double dielectric barrier discharges at atmospheric pressure," *J. Appl. Phys.*, vol. 120, no. 11, p. 114901, Sep. 2016.

[18] W. V. Gaens and A. Bogaerts, "Kinetic modelling for an atmospheric pressure argon plasma jet in humid air," *J. Phys. Appl. Phys.*, vol. 46, no. 27, p. 275201, 2013.